Front. Environ. Sci. Eng. 2020, 14(6): 108
https://doi.org/10.1007/s11783-020-1287-0

RESEARCH ARTICLE

Influences and mechanisms of nanofullerene on the horizontal transfer of plasmid-encoded antibiotic resistance genes between *E. coli* strains

Qingkun Ji[1], Caihong Zhang (✉)[2], Dan Li (✉)[1]

1 Shanghai Key Laboratory of Atmospheric Particle Pollution and Prevention (LAP[3]), Department of Environmental Science and Engineering, Fudan University, Shanghai 200433, China

2 Department of Obstetrics and Gynecology, Changhai Hospital, Second Military Medical University, Shanghai 200433, China

HIGHLIGHTS

- Sub-inhibitory levels of nC_{60} promote conjugative transfer of ARGs.
- nC_{60} can induce ROS generation, oxidative stress and SOS response.
- nC_{60} can increase cell membrane permeability and alter gene expression.
- Results provide evidence of nC_{60} promoting antibiotic resistance dissemination.

GRAPHIC ABSTRACT

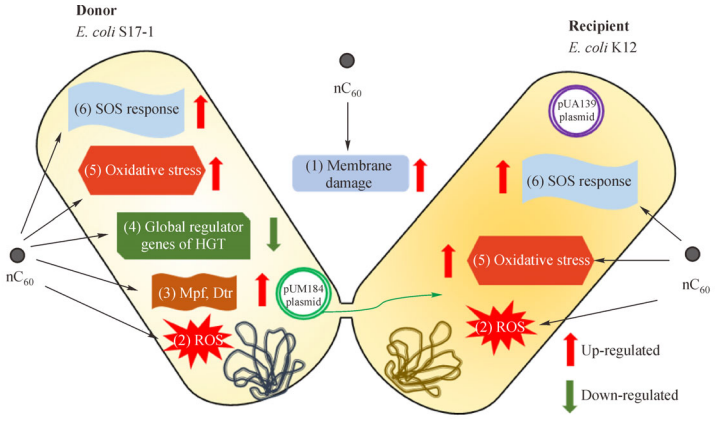

ARTICLE INFO

Article history:
Received 6 January 2020
Revised 6 May 2020
Accepted 11 May 2020
Available online 19 June 2020

Keywords:
Nanofullerene
Sub-minimum inhibitory concentrations
Antibiotic resistance genes
Conjugation
Molecular biological techniques

ABSTRACT

The spread and development of antibiotic resistance globally have led to severe public health problems. It has been shown that some non-antibiotic substances can also promote the diffusion and spread of antibiotic resistance genes (ARGs). Nanofullerene (nC_{60}) is a type of nanomaterial widely used around the world, and some studies have discovered both the biological toxicity and environmental toxicity of nC_{60}. In this study, cellular and molecular biology techniques were employed to investigate the influences of nC_{60} at sub-minimum inhibitory concentrations (sub-MICs) on the conjugation of ARGs between the *E. coli* strains. Compared with the control group, nC_{60} significantly increased the conjugation rates of ARGs by 1.32−10.82 folds within the concentration range of 7.03−1800 μg/L. This study further explored the mechanism of this phenomenon, finding that sub-MICs of nC_{60} could induce the production of reactive oxygen species (ROS), trigger SOS-response and oxidative stress, affect the expression of outer membrane proteins (OMPs) genes, increase membrane permeability, and thus promote the occurrence of conjugation. This research enriches our understanding of the environmental toxicity of nC_{60}, raises our risk awareness toward nC_{60}, and may promote the more rational employment of nC_{60} materials.

1 Introduction

Antibiotic resistance is regarded as one of the biggest worldwide public health problems of the twenty-first

✉ Corresponding authors
E-mail: 13817194198@126.com (C. Zhang); lidanfudan@fudan.edu.cn (D. Li)

Century (WHO, 2017), and has been ranked as one of the six new environmental problems in the whole world by the United Nations Environment Programme (UNEP, 2017; Vikesland et al., 2019). It is estimated that more than 700000 people died annually because of infections caused by antibiotic resistant bacteria (Wang et al., 2019). Horizontal gene transfer is considered to be the most important driver for bacteria to acquire and spread ARGs, and is mainly implemented in three manners: conjugation, transformation and transduction (Andersson and Hughes, 2010).The misuse and abuse of antibiotics in hospitals and in agriculture are recognized as the predominant reasons for the development and spread of ARGs (Thomas and Nielsen, 2005; Yu et al., 2019). However, some non-antibiotic chemicals, such as disinfectants (Zhang et al., 2017), non-antibiotic drugs (Wang et al., 2019), metal ions, and nano metal oxides (Nguyen et al., 2019; Zhang et al., 2019), can also facilitate the development and diffusion of ARGs.

Fullerene (C_{60}), which was discovered in 1985, has been extensively studied due to its unique physical and chemical characteristics (Bezzu et al., 2019; Tan et al., 2019). The wide application of C_{60} in electronics, medicine, and cosmetics has contributed to its emission and accumulation in various environments, which leads to the increasing exposure opportunities for microorganisms (Thauvin et al., 2008; Castro et al., 2017). It has been reported that the concentration of C_{60} in sewage treatment plants can reach 19 μg/L (Farré et al., 2010). Many studies have paid attention to the toxicity of C_{60}, which can induce ROS, and subsequent oxidative damage to cell membranes and DNA (Nel et al., 2009). However, the influences and mechanisms of C_{60} on the occurrence and migration of ARGs at environmentally relevant concentrations are still unclear.

To address this knowledge gap, we performed experiments on the influences of nC_{60} on the transformation and conjugation of plasmid-encoded ARGs and probed the underlying mechanisms. The results of this study provide a new perspective into the spread of antibiotic resistance exposure to environmental levels of nC_{60}, and have great significance for guiding the application of nC_{60} materials and other nanomaterials in the future.

2 Materials and methods

2.1 Donor and recipient strains, antibiotic resistant plasmid, and culture conditions

As the most representative gram-negative model microorganism, *E. coli* was employed to appraise the conjugation as our previous studies reported (Zhang et al., 2017). *E. coli* S17-1 was selected as the donor strain, which contained a movable plasmid pCM184-Cm (7625bp) and was regulated by the RP4 DNA segment of the host's chromosomes (Zhang et al., 2017). Chloramphenicol (Chl) resistance gene was encoded by the pCM184-Cm plasmid. The recipient strain, *E. coli* K12, contained immovable plasmids pUA139, carrying kanamycin (Km) resistance genes. Culture conditions for bacterial strains were cultured in Luria-Bertani (LB) liquid medium (100 μg/mL Km or 20 μg/mL Chl, respectively) at 37°C with 180 r/min shaking. The overnight-cultured strains were used in the following experiments. Text S1 exhibited more information on the media, antibiotics and other reagents in the supported information (SI).

2.2 Preparation and characterization of nC_{60} solution

Preparation of nC_{60} solution was conducted referring to previous studies (Yin et al., 2016). Briefly, 4.0 mg of C_{60}, 18 mL of toluene, and 144 mL of ultrapure water were heterogeneously mixed in a sealed bottle using an ultrasonic instrument (Xinzhi, China). The stock solution afterwards was filtered using a 0.45 μm Teflon filter, and the concentration of nC_{60} solution was measured by ultraviolet absorption at 334 nm, which was 7200 μg/L in the present study. The particle size of nC_{60} was determined by Malvern Instruments nanoparticle size-Zeta potentiometric analyzer (ZS90, the UK). The detailed protocol is illustrated in Text S2 of the SI.

2.3 Determination of the sub-MICs of nC_{60}

According to previous studies (Zhang et al., 2019), the sub-MICs were determined to evaluate the effect of nC_{60} on *E. coli* microbial activity. In short, the overnight culture of *E. coli* was diluted in the ratio of 1:100 into the LB liquid medium and added into 96-orifice plate with 100 μL per well. Then, the nC_{60} was added into a 96-orifice plate by serial dilution (twofold) method. After 16−18 h culture at 37°C, we measured the optical density at 600 nm (OD_{600}) by using a microplate reader. Then the OD_{600} value was used to calculate the inhibition rate and each experiment should be done in triplicate.

2.4 Influences of nC_{60} on the conjugation and transformation of plasmid-encoded ARGs

In this study, an optimized conjugation model was applied to evaluate the influence of nC_{60} on the conjugation of ARGs between different *E. coli* strains referring to the previous publication (Zhang et al., 2018). First, the overnight cultured *E. coli* strains were centrifuged for 4−5 min at 8000 r/min and washed using phosphate buffer saline (PBS). Then, the donor and receipt *E. coli* strains were resuspended in PBS at a concentration of approximately 10^8 CFU/mL and mixed at a proportion of 1.5:1 for further conjugation experiments. Then, the control group and the experimental groups were treated with various concentrations of nC_{60} and PBS, and then incubated at

37°C for 240 min. The nC_{60} treated experimental groups and the control groups were coated onto different LB solid plates with different antibiotics to detect the concentrations of the donor *E. coli* S17-1, recipient *E. coli* K12, and transconjugants. Finally, both the ratio of nC_{60} to the conjugation rate of ARGs (the ratio of the concentrations of transconjugants to the concentrations of recipient strains) and the conjugation rate relative to the control group were calculated. Meanwhile, in order to prove the role of ROS in the conjugation, an experiment was conducted with Thiourea (TU, ROS scavenger). In this experiment, TU (a final concentration of 100 mmol/L) and various concentrations of nC_{60} were added to the PBS. Afterwards, the conjugation rates with and without TU were compared. Each experiment, independently, was carried out in triplicate.

In addition, an optimized transformation model was also constructed to assay whether nC_{60} has an impact on uptake of ARGs gene via transformation (Ding et al., 2016). In short, *E. coli* was cultured overnight and treated under certain conditions for a period of time. To calculate the transformation rate, the culture was mixed with plasmids, plated onto LB agar plates, and then counted. The detailed protocol is explained in Text S3 in of the SI.

2.5 Determination of intracellular ROS (intra-ROS) levels induced by nC_{60}

Intra-ROS in *E. coli* exposed to nC_{60} was measured via a fluorescent probe DCFH-DA assay referring to previous research (Zhang et al., 2018). The overnight-cultured *E. coli* was washed and resuspended in PBS. After that, the DCFH-DA probes with final consistence of 10 μmol/L were put into the bacterial suspension, and then the mixtures were incubated avoiding light for 20 min at 37°C, and being shaken every 3−5 min. After using the PBS to wash away the extracellular DCFH-DA probes, nC_{60} was used to treat the *E. coli*. The bacterial solution was then moved to a 96-orifice plate, and a microplate reader was used to gauge the Fluorescence Intensity (excitation and emission wavelengths were 488 and 525 nm, respectively). The intra-ROS levels were compared between the experimental and control groups. Each experiment, independently, was carried out in triplicate.

2.6 Influences of nC_{60} on bacterial cell membrane

The effect of nC_{60} on the cell membrane permeability (CMP) of *E. coli* was assessed using propidium iodide (PI) and flow cytometry (FCM) (Wang et al., 2019). Each experiment, independently, was carried out in triplicate. PI is a cell nucleus stain for DNA staining, and we could characterize the permeability degree of cell membranes according to the intensity of the generated fluorescence. 0.5 mL bacterial solution treated in nC_{60} and 0.5 mL blank control bacterial solution were respectively taken, and their concentration was approximately 10^8 CFU/mL. PI (with the final concentration of 30 μmol/L) was added to both of them for staining. These bacterial solutions were placed in the dark for 15 min and tested with FCM. Some parameters of FCM were set as follows: excitation, emission and lateral angular scattered wavelengths were 488 nm, 653−669 nm, and 483−493 nm, respectively. BD CellQuest software (BD Biosciences, USA) was applied to obtain data from 100,000 cells tested at a single time and perform data analysis.

The influences of nC_{60} on the morphology and membrane surface structures of both donor and recipient *E. coli* were observed using a transmission electron microscopy (TEM) (Zhang et al., 2018). The donor and recipient conjugative mixtures (approximately 10^8CFU/mL), exposure to various concentrations of nC_{60} for 240 min, as well as the control groups, were respectively placed onto copper grids, and then left dry naturally. Finally, all the samples were detected and photographed by TEM (JEM-2100F, Japan) at 75 kV, and the pictures were processed by RADIUS (EMSIS, Germany).

2.7 Gene expressions induced by nC_{60} detected by quantitative RT-PCR

The expression of conjugation genes, including global regulator genes (*trbA, korA*, and *korB*), DNA transfer and replication (Dtr) system genes (*traJ* and *trfAp*), mating pair formation (Mpf) system genes (*traF* and *trbBp*), SOS-response genes (*umuD, recA*, and *lexA*), oxidative stress genes (*rpoS, oxyR, soxR* and *soxS*), and outer membrane proteins (OMPs) genes (*ompF, ompA* and *ompC*), were evaluated using quantitative RT-PCR, and the 16S rRNA fragment was employed as an internal reference (Zhang et al., 2018). The detailed protocol of RNA extraction and quantification is illustrated in Text S4 of the SI. The RT-PCR was performed in a PCR instrument (CFX 96, Bio-Rad, Hercules, CA, USA) using SYBR Green I. The RT-PCR mixture consisted of 2.5 μL of 2 × SYBR Premix Ex Taq, 0.1 μL of each primer (at the final concentration of 10 μmol/L), 0.5 μL cDNA template, and 1.8 μL of distilled water. The amplification reaction conditions included incubation at 95°C for 30 s for predegeneration, further incubation at 95°C for 45 s for degeneration, and then annealing at 60°C for 45 s, which took a total of 40 cycles. After the amplification reaction was completed, analysis of the melting curves was conducted at 95°C for 15 s and at 60°C for 60 s. Table S5 presents the primer sequences used in present study.

2.8 Statistical analysis

The data were analyzed by SPSS. Variance analysis (ANOVA) was employed to statistically evaluate the significance of the data. The results were considered significant if $P < 0.05$ (*), quite significant if $P < 0.01$

(**), and extremely significant if $P < 0.001$ (***) (Zhang et al., 2018).

3 Results and discussion

3.1 Cytotoxicity of nC_{60}

The particle size distribution of the nC_{60} solution prepared in this study was between 100 nm and 400 nm, predominantly around 200 nm (Figure S1) (Alargova et al., 2001). The concentration of the nC_{60} stock solution was 7200 μg/L. Although the solubility of C_{60} is less than 10^{-6} μg/L in water (Andrievsky et al., 1999), the aggregation property of C_{60} in solvents makes it easy for C_{60} nanocrystalline particles to form (5−500 nm) in water, which is 11 orders of magnitude higher than that of the molecular solubility (Alargova et al., 2001). The inhibitory effect of nC_{60} against *E. coli* was determined, and the results indicated that EC50 (50% inhibitory efficiency) was approximately 3600 μg/L (Table S1). The sub-MICs of nC_{60} tested in present study (Table S2) were chosen referring to EC50 measured in this study, minimal inhibitory concentrations (MICs) from previous studies (500 to 1000 μg/L) (Lyon et al., 2005), and the detected environmental concentrations (19 μg/L) (Farré et al., 2010).

3.2 The influence of nC_{60} on transformation and conjugation

nC_{60} promoted conjugation in a concentration-dependent (0.44 to 1800 μg/L) manner, increasing the conjugation rate by 1.3−10.8 folds compared with the control group (Fig. 1, S2, and Table S3). The efficiency of conjugation was approximately 5.1×10^{-5} spontaneously, which was basically the same as the previous research (Zhang et al., 2017). Previous studies also found that metal nanoparticles and ions could accelerate the horizontal transfer in a concentration-dependent pattern (Zhang et al., 2019). Additionally, the results demonstrated that nC_{60} did not induce plasmid-mediated ARGs transformation in *E. coli* K12 and the plasmid could be transferred into the receptive cells (Table S4). Recipient cells not treated with Ca^{2+} did not have the ability to obtain plasmids. Therefore, we observed the failure of transformation. Taken together, our results showed that nC_{60}, at sub-MICs, can facilitate the transmission of plasmid-carried ARGs via conjugation but not transformation. This finding implies that the widespread occurrence of nonmetal nanoparticles may influence the dissemination of ARGs.

3.3 Mechanisms underlying the facilitated horizontal transfer of ARGs by nC_{60}

Considerable evidence has suggested that the ROS formation plays a critical role in the toxicity of nanoparticles (Zhang et al., 2019). As a consequence, we hypothesized that the formation of intra-ROS, following increases in CMP, stimulation of oxidative stress, DNA damage and repair, SOS-response, and alterations of conjugation-related genes expression caused by nC_{60}, may promote the horizontal transfer of plasmid-encoded ARGs.

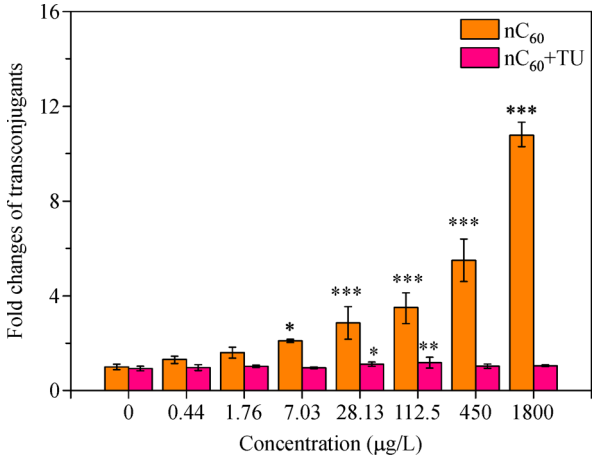

Fig. 1 Fold changes between *E. coli* strains in conjugation frequency upon exposure to nC_{60}. nC_{60} had significant influences on the conjugation of plasmid-encoded ARGs (ANOVA, $P < 0.05$). Significant differences between nC_{60} + TU or individual nC_{60} treated groups and the control (0 μg/L of nC_{60}) were tested with ANOVA (LSD).

3.3.1 Influence of nC_{60} on the formation of intra-ROS

Intra-ROS comprises highly reactive molecules, including nonspecific hydroxyls (·OH), superoxides (O_2·), and hydrogen peroxide (H_2O_2), which can react with biological molecules and thus disturb a range of cellular components and physiologic processes (Imlay, 2003). As shown in Fig. 2, the intra-ROS levels in the recipient and donor cells clearly promoted with the growing nC_{60} consistence (Figs. 2(a) and 2(b)). With increasing nC_{60} concentrations (0.44–1800 μg/L), the intra-ROS levels of *E. coli* K12 and *E. coli* S17 improved by 1.59–2.89, 1.35–3.13 folds that of the control group, respectively (Figs. 2(a) and 2(b)). The presence of an ROS scavenger markedly decreased the rates of conjugation (Fig. 1), which implied that intra-ROS generated by nC_{60} stimulated or was related to the enhanced conjugation of ARGs. Furthermore, the levels of intra-ROS formation and the conjugative frequencies exhibited significant positive correlations ($P < 0.05$), with an R^2 of 0.9166 for the donor *E. coli* and 0.8408 for the recipient *E. coli* (Figs. 2(c) and 2(d)). Thus far, we have confirmed that nC_{60} induces intra-ROS, thereby promoting the intragenera conjugation of ARGs. Intra-ROS can induce oxidation, which leads to damage of cellular components and, finally, death of bacterial strains (Han

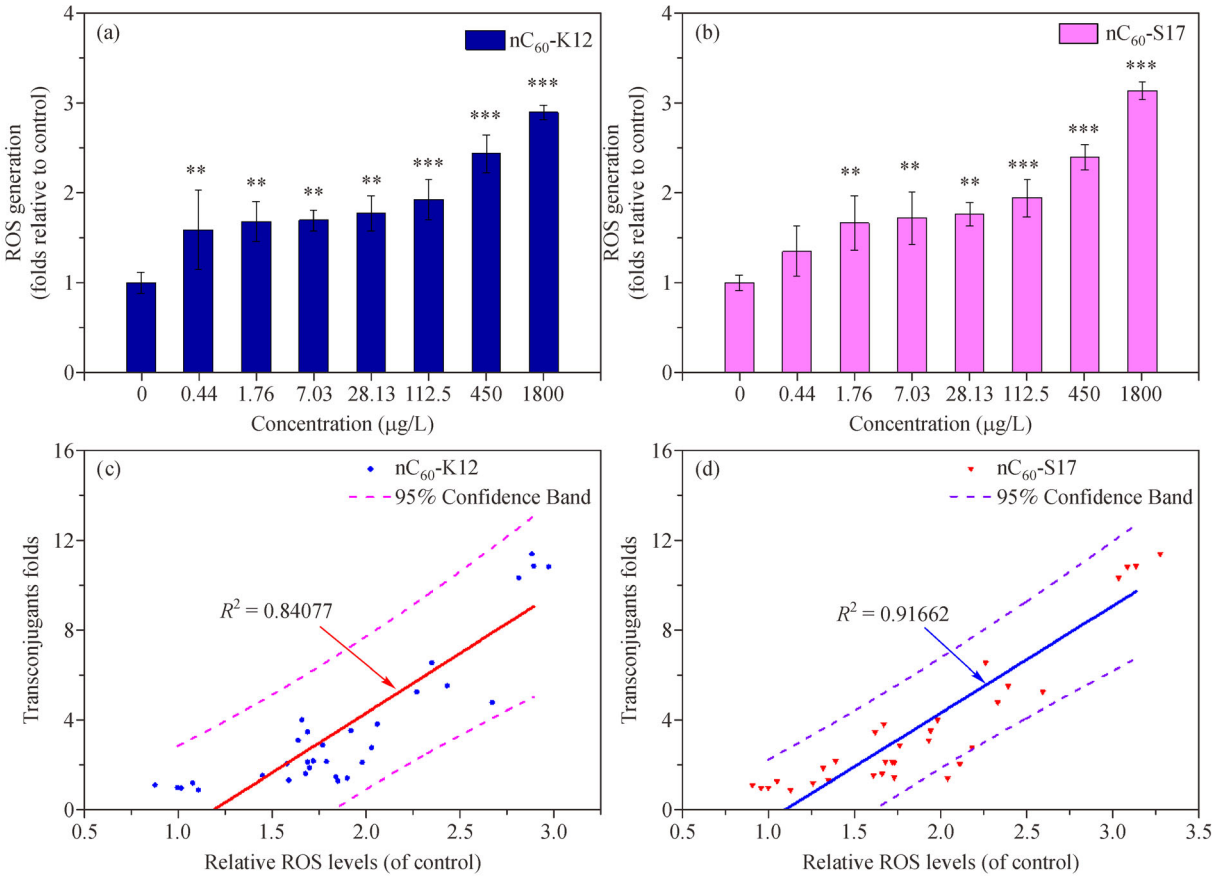

Fig. 2 Exposure to nC_{60} increases intra-ROS formation that significantly correlates with conjugation of plasmid-encoded ARGs. The intra-ROS levels in *E. coli* K12 (a) and *E. coli* S17 (b) induced by nC_{60}. Correlations between the conjugation rates (fold changes) and intra-ROS formation levels (fold changes) in *E. coli* K12 (c) and *E. coli* S17 (d). Significant differences between the non-exposed control group and nC_{60}-exposed groups were tested with ANOVA (LSD).

et al., 2013; Zhang et al., 2019). Recent evidence implied that sub-MICs levels of nanoparticles could increase the conjugation of ARGs by stimulating the generation of intra-ROS in donor and recipient cells, altering the tRNA synthetase, inducing DNA damage and mutagenesis, and inducing multidrug efflux systems (Zhang et al., 2019).

3.3.2 Influence of nC_{60} on CMP

To explore whether nC_{60} increases CMP, flow cytometry was used to evaluate the CMP of the donor and recipient strains. The experimental results (Fig. S3) showed that the CMP of the donor *E. coli* S17 and the recipient *E. coli* K12 in the control group were 6.71% and 4.74%, respectively. As the nC_{60} concentration rose, the CMP of the donor and the recipient strains also increased. When the nC_{60} concentration was 450 μg/L and 1800 μg/L, the CMP of the recipient *E. coli* K12 strains was 6.73% and 21.51%, respectively, and the CMP of the donor *E. coli* S17 strains was 7.18% and 21.69%, respectively (Fig. S3).

To observe damage of the cell membrane, we used TEM to image *E. coli.* The results indicated that the surface of the control group (without nC_{60} treatment) was smooth and complete (Fig. 3(b)), while the cell membrane of *E. coli* exposed to nC_{60} was rough or even broken (Figs. 3(c) and 3(d)). nC_{60} exposure can damage the cell membrane to varying degrees. Similarly, the addition of nano materials increased the permeability of the cell membrane and damaged it (Zhang et al., 2019).

3.3.3 Influence of nC_{60} on the expression of genes related with the oxidative stress, SOS-response, outer membrane protein and conjugation

To further explore the molecular mechanism of the influence of nC_{60} on conjugation, we used quantitative RT-PCR to quantify the expression of 17 genes related to the SOS-response, oxidative stress, outer membrane, and conjugation, and the results indicated that the expression of these genes was significantly impacted, with increasing nC_{60} concentrations (0.44−1800 μg/L) (Figs. 4 and 5).

As nC_{60} could induce intra-ROS, nC_{60} could accord-

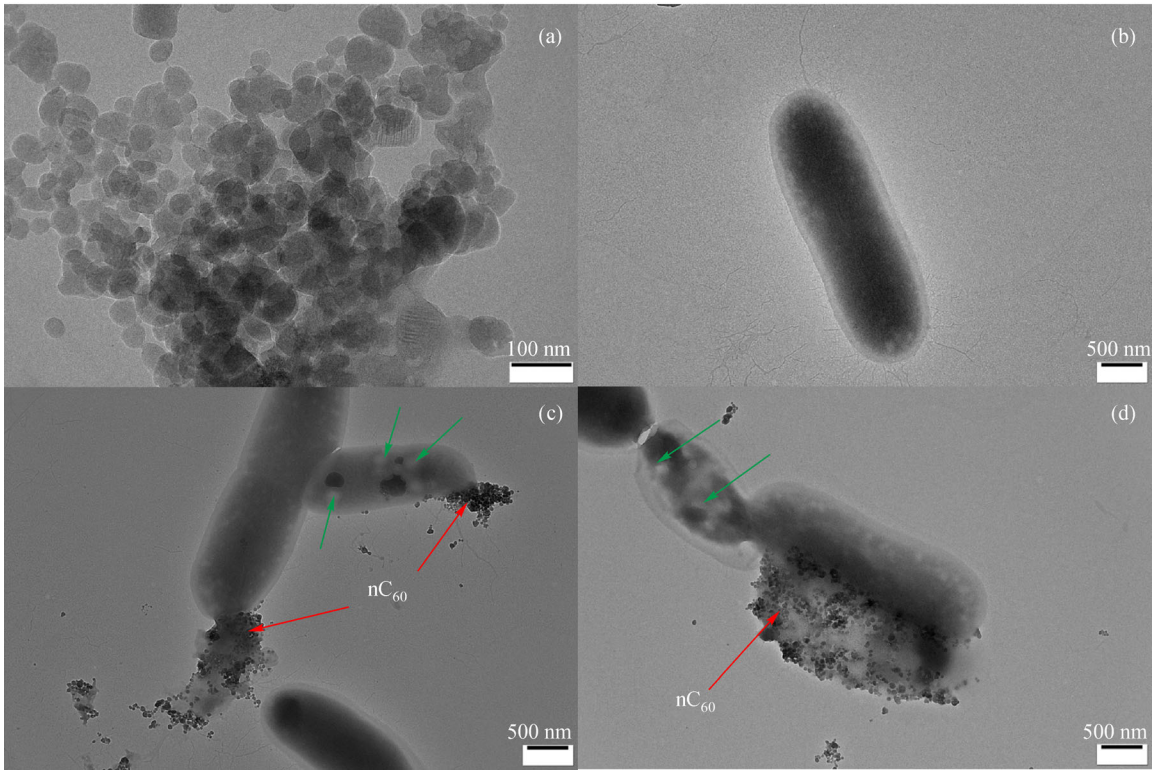

Fig. 3 TEM pictures of nC_{60} (a), *E. coli* in the test group (no nC_{60} exposure) (b), *E. coli* afterwards exposure to nC_{60} (450 μg/L) (c), and *E. coli* after exposure to nC_{60} (1800 μg/L) (d). The red arrows refer to nC_{60} and the green arrows refer to the pores formed after exposure to nC_{60}.

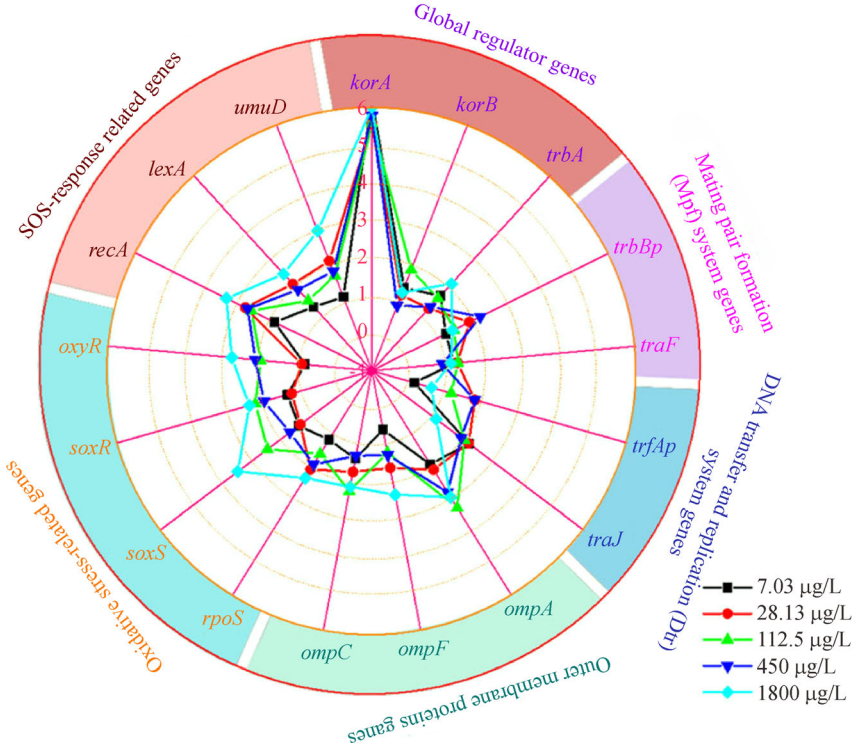

Fig. 4 Impacts of nC_{60} on the mRNA expression levels of genes involved in the OMPs, Global regulation, Oxidative stress, Mpf system, SOS-response, and Dtr system during conjugation. The radial axis depicts the $\log_2$-fold absolute values of genes relative to the control group.

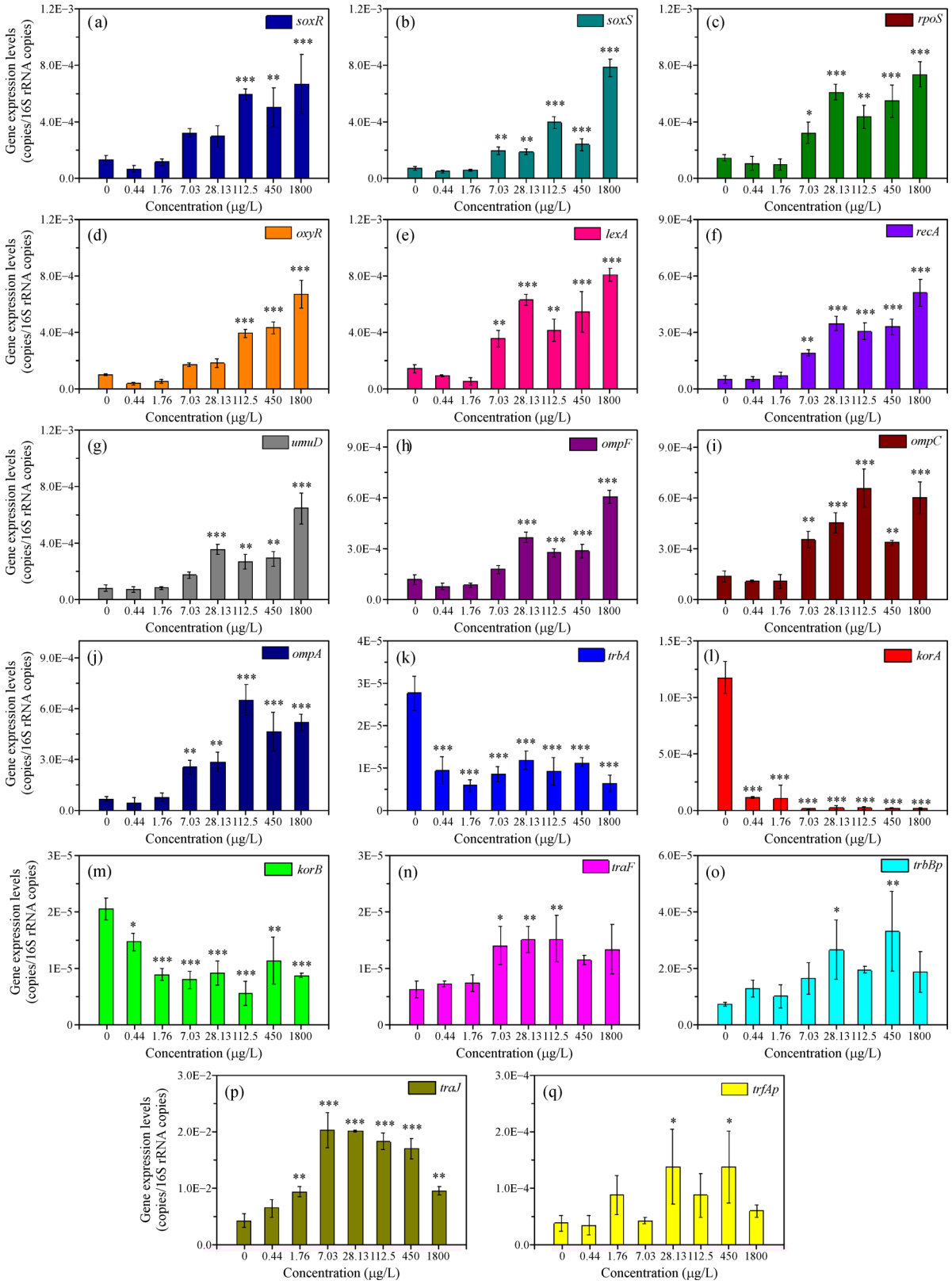

Fig. 5 Impacts of nC_{60} on the mRNA expression levels of genes involved in *soxR* (a), *soxS* (b), *rpoS* (c), *oxyR* (d), *lexA* (e), *recA* (f), *umuD* (g), *ompF* (h), *ompC* (i), *ompA* (j), *trbA* (k), *korA* (l), *korB* (m), *traF* (n), *trbBp* (o), *traJ* (p), and *trfAp* (q), during conjugation. Significant differences between the non-exposed control group and nC_{60}-exposed groups were tested with ANOVA (LSD).

ingly induce oxidative stress, DNA damage, and then the SOS-response (Figs. 2, 4, and 5). The expression of genes involved in the oxidative stress pathway (*soxR, soxS*, *rpoS*, and *oxyR*) (Figs. 5(a)−(d)), and SOS-response (*lexA, recA*, and *umuD*) (Figs. 5(e)−(g)) were upregulated when nC_{60} concentrations increased. The maximum upregulation of *soxR, soxS*, *rpoS*, *oxyR, lexA, recA*, and *umuD* was 5.17, 10.88, 5.11, 6.6, 5.54, 9.84, and 7.87 folds that of the control group, respectively (Fig. 5(a)−5(g)). ROS production can induce the regulation of RpoS protein, which may stimulate oxidative stress and the SOS-response (Andersson and Hughes, 2014). Many studies have shown that the SOS-response is related to the conjugation of genes (Zhang et al., 2018). The expressions of *lexA* and *recA* genes are increased when DNA damage occurs and then the SOS-response is activated (Zhang et al., 2018). For *E. coli*, SoxRS and OxyR transcription factors activate the antioxidant defense system of *E. coli*, which is closely related to the oxidative stress response, and SoxRS is primarily composed of two transcribed *soxR* and *soxS* regulator genes (Kabir and Shimizu, 2006). Therefore, the expression of genes in the oxidative stress pathway and SOS-response were upregulated, which enhanced horizontal transfer.

OmpC (36 kDa), OmpF (35 kDa), and OmpA (34 kDa), are three types of OMPs that are closely related to the permeability of bacterial cell membranes and play a critical role in the formation of membrane pores and horizontal transfer of genes (Koebnik et al., 2000). The present results indicated that the expression of OMPs genes (*ompF*, *ompC*, and *ompA*) (Figs. 5(h)−5(j)) increased as the nC_{60} concentration was enhanced. The maximum upregulation of *ompA*, *ompF* and *ompC* was 9.74, 5.1, and 4.8 folds that of the control group, respectively (Figs. 5(h)−5(j)). The subsequent increase of *ompA* and *ompC* could augment CMP via pore forming and the membrane transport of plasmid-encoded ARGs (Zhang et al., 2018). The TEM results showed that the bacterial outer membrane was impaired, and pores were formed due to exposure to nC_{60} (Fig. 3), which may enhance the transfer of resistance plasmids between two different *E. coli*. This phenomenon was similar to the result of diesel and petrol exhaust particles accelerating horizontal transfer (Zhang et al., 2018).

With increasing nC_{60} concentrations (0.44−1800 μg/L), the expression of genes (*trbA, korA*, and *korB*) in global regulatory system was significantly downregulated (Figs. 5(k)−5(m)). The maximum downregulation of *korA*, *korB,* and *trbA* was 99%, 73%, and 79% compared with the control group, respectively. Exposure to nC_{60} resulted in a significant increase in the gene expression of the Mpf system genes (*traF* and *trbBp*) (Figs. 5(n) and 5(o)) and the Dtr system genes (*traJ* and *trfAp*) (Fig. 5(p) and 5(q)). The expression of *traJ*, *traF*, *trfAp*, and *trbBp* genes was upregulated by 1.5−4.65, 1.16−2.44, 0.9−3.56, and 1.4−4.59 folds compared with the control group, respectively. (Figs. 5(n)−5(q)). The completion of conjugation first requires the formation of a conjugative bridge between the recipient and donor strains, and this process requires the involvement of global regulatory genes, Dtr system genes, and Mpf system genes (Zhang et al., 2018). The Mpf system genes are recognized as critical factors in conjugation (Eisenbrandt et al., 2000), while the down-regulation of global regulatory genes plays a pivotal role in Mpf system genes (Schröder and Lanka, 2005). The Mpf system is to the benefit of the formation of the membrane-related channels and proteins that are important passageways for single-stranded DNA metastasis (Zhang et al., 2017). TraF protein is an important proteins for pilus assembly, and its expression levels are positively related to horizontal gene metastasis among different *E.coli* (Sakai and Komano, 1996). Genes in the Dtr system can facilitate conjugation (Zhang et al., 2018), and *traJ* gene expression is also affected by global regulatory genes (Sakai and Komano, 1996). The expression of *korB* and *korA* genes jointly inhibits the expression of *trbBp* gene, while the expression of *trbA* and *korB* genes jointly inhibits the expression of *trfAp* gene. The study results show that nC_{60} significantly inhibits the expression of *trbA*, *korA,* and *korB* gene (Kostelidou et al., 1999), thus promoting the expression of *trfAp* and *trbBp* genes and further contributing to the formation of a conjugative bridge between donor and recipient strains. Qiu et al. have shown similar results (Qiu et al., 2012).

In general, nC_{60} leads to intra-ROS production, resulting in cell membrane damage. Therefore, it increases the CMP or contributes to the formation of a conjugative bridge, leading to the conjugation of ARGs in *E. coli*.

4 Conclusions

This study verified that nC_{60} at sub-MICs can facilitate the conjugation of plasmid-harboring ARGs, thereby possibly promoting the spread and development of antimicrobial resistance in the natural environment. The underlying mechanisms have been explored by using biochemical, physiologic, and molecular techniques, which involve production of intra-ROS, increasing the CMP, stimulating oxidative stress and the SOS-response, and regulating the expression of genes related to conjugation. This study provides proof of the ecological influence of low levels of nanoparticles on antimicrobial resistance and underscores the urgency of strengthening efficacious policies and technologies to control nanoparticles in environments.

Acknowledgements This work was supported by grants from the National Natural Science Foundation of China (Grant Nos. 91843301, 21527814 and 91643106).

Electronic Supplementary Material Supplementary material is available in the online version of this article at https://doi.org/10.1007/s11783-020-1287-0 and is accessible for authorized users.

References

Alargova R G, Deguchi S, Tsujii K (2001). Stable colloidal dispersions of fullerenes in polar organic solvents. Journal of the American Chemical Society, 123(43): 10460–10467

Andersson D I, Hughes D (2010). Antibiotic resistance and its cost: Is it possible to reverse resistance? Nature Reviews. Microbiology, 8(4): 260–271

Andersson D I, Hughes D (2014). Microbiological effects of sublethal levels of antibiotics. Nature Reviews. Microbiology, 12(7): 465–478

Andrievsky G V, Klochkov V K, Karyakina E L, Mchedlov-Petrossyan N O (1999). Studies of aqueous colloidal solutions of fullerene C_{60} by electron microscopy. Chemical Physics Letters, 300(3–4): 392–396

Bezzu C G, Burt L A, Mcmonagle C J, Moggach S A, Kariuki B M, Allan D R, Warren M, Mckeown N B (2019). Highly stable fullerene-based porous molecular crystals with open metal sites. Nature Materials, 18(7): 740–745

Castro E, Hernandez Garcia A, Zavala G, Echegoyen L (2017). Fullerenes in biology and medicine. Journal of Materials Chemistry B, 5(32): 6523–6535

Ding C, Pan J, Jin M, Yang D, Shen Z, Wang J, Zhang B, Liu W, Fu J, Guo X, Wang D, Chen Z, Yin J, Qiu Z, Li J (2016). Enhanced uptake of antibiotic resistance genes in the presence of nanoalumina. Nanotoxicology, 10(8): 1051–1060

Eisenbrandt R, Kalkum M, Lurz R, Lanka E (2000). Maturation of IncP Pilin precursors resembles the catalytic dyad-like mechanism of leader peptidases. Journal of Bacteriology, 182(23): 6751–6761

Farré M, Pérez S, Gajda-Schrantz K, Osorio V, Kantiani L, Ginebreda A, Barceló D (2010). First determination of C_{60} and C_{70} fullerenes and *N*-methylfulleropyrrolidine C_{60} on the suspended material of wastewater effluents by liquid chromatography hybrid quadrupole linear ion trap tandem mass spectrometry. Journal of Hydrology (Amsterdam), 383(1–2): 44–51

Han S, Lemire J, Appanna V P, Auger C, Castonguay Z, Appanna V D (2013). How aluminum, an intracellular ROS generator promotes hepatic and neurological diseases: the metabolic tale. Cell Biology and Toxicology, 29(2): 75–84

Imlay J A (2003). Pathways of oxidative damage. Annual Review of Microbiology, 57(1): 395–418

Kabir M M, Shimizu K (2006). Investigation into the effect of *soxR* and *soxS* genes deletion on the central metabolism of *Escherichia coli* based on gene expressions and enzyme activities. Biochemical Engineering Journal, 30(1): 39–47

Koebnik R, Locher K P, Van Gelder P (2000). Structure and function of bacterial outer membrane proteins: barrels in a nutshell. Molecular Microbiology, 37(2): 239–253

Kostelidou K, Jones A C, Thomas C M (1999). Conserved C-terminal region of global repressor korA of broad-host-range plasmid RK2 is required for co-operativity between *korA* and a second RK2 global regulator, *korB*. Journal of Molecular Biology, 289(2): 0–221

Lyon D Y, Fortner J D, Sayes C M, Colvin V L, Hughes J B (2005). Bacterial cell association and antimicrobial activity of a C60 water suspension. Environmental Toxicology and Chemistry, 24(11): 2757–2762

Nel A E, Madler L, Velegol D, Xia T, Hoek E M, Somasundaran P, Klaessig F, Castranova V, Thompson M (2009). Understanding biophysicochemical interactions at the nano-bio interface. Nature Materials, 8(7): 543–557

Nguyen C C, Hugie C N, Kile M L, Navab-Daneshmand T (2019). Association between heavy metals and antibiotic-resistant human pathogens in environmental reservoirs: A review. Frontiers of Environmental Science & Engineering, 13(3): 46

Qiu Z, Yu Y, Chen Z, Jin M, Yang D, Zhao Z, Wang J, Shen Z, Wang X, Qian D, Huang A, Zhang B, Li J W (2012). Nanoalumina promotes the horizontal transfer of multiresistance genes mediated by plasmids across genera. Proceedings of the National Academy of Sciences of the United States of America, 109(13): 4944–4949

Sakai H, Komano T (1996). DNA replication of *IncQ* broad-host-range plasmids in gram-negative bacteria. Bioscience, Biotechnology, and Biochemistry, 60(3): 377–382

Schröder G, Lanka E (2005). The mating pair formation system of conjugative plasmids-A versatile secretion machinery for transfer of proteins and DNA. Plasmid, 54(1): 1–25

Tan Z, Zhang D, Tian H R, Wu Q, Hou S, Pi J, Sadeghi H, Tang Z, Yang Y, Liu J, Tan Y Z, Chen Z B, Shi J, Xiao Z, Lambert C, Xie S Y, Hong W (2019). Atomically defined angstrom-scale all-carbon junctions. Nature Communications, 10(1): 1748

Thauvin C, Rickling S, Schultz P, Celia H, Meunier S, Mioskowski C (2008). Carbon nanotubes as templates for polymerized lipid assemblies. Nature Nanotechnology, 3(12): 743–748

Thomas C M, Nielsen K M (2005). Mechanisms of, and barriers to, horizontal gene transfer between bacteria. Nature Reviews. Microbiology, 3(9): 711–721

UNEP (2017). Frontiers 2017: Emerging Issues of Environmental Concern. Geneva: United Nations Environment Programme

Vikesland P, Garner E, Gupta S, Kang S, Maile-Moskowitz A, Zhu N (2019). Differential drivers of antimicrobial resistance across the world. Accounts of Chemical Research, 52(4): 916–924

Wang Y, Lu J, Mao L, Li J, Yuan Z, Bond P L, Guo J (2019). Antiepileptic drug carbamazepine promotes horizontal transfer of plasmid-borne multi-antibiotic resistance genes within and across bacterial genera. ISME Journal, 13(2): 509–522

WHO (2017). Global Health Case Challenge: fighting antibiotic resistance. Geneva: World Health Organization

Yin L, Zhou H, Lian L, Yan S, Song W (2016). Effects of C_{60} on the photochemical formation of reactive oxygen species from natural organic matter. Environmental Science & Technology, 50(21): 11742–11751

Yu Y, Zhu X, Wu G, Wang C, Yuan X (2019). Analysis of antibiotic resistance of *Escherichia coli* isolated from the Yitong River in North-east China. Frontiers of Environmental Science & Engineering, 13(3): 39

Zhang S, Wang Y, Song H, Lu J, Yuan Z, Guo J (2019). Copper nanoparticles and copper ions promote horizontal transfer of plasmid-mediated multi-antibiotic resistance genes across bacterial genera. Environment International, 129: 478–487

Zhang Y, Gu A Z, Cen T, Li X, Li D, Chen J (2018). Petrol and diesel exhaust particles accelerate the horizontal transfer of plasmid-

mediated antimicrobial resistance genes. Environment International, 114: 280–287

Zhang Y, Gu A Z, He M, Li D, Chen J (2017). Subinhibitory concentrations of disinfectants promote the horizontal transfer of multidrug resistance genes within and across genera. Environmental Science & Technology, 51(1): 570–580